

Investigation of ground level magnetic field disturbances after the 2010 Chile 8.8M and 2015 Chile 8.3M earthquakes

P.A. Inchin,⁽¹⁾ M.D. Zettergren,⁽¹⁾ J.B. Snively,⁽¹⁾ A. Komjathy,⁽²⁾ O. Verkhoglyadova⁽²⁾

(1) Embry-Riddle Aeronautical University, Daytona Beach, FL, USA
(2) Jet Propulsion Laboratory, California Institute of Technology, Pasadena, CA, USA
E-mail: inchinp@my.erau.edu

Abstract: Recent scientific reports have identified geomagnetic field perturbations likely due to acoustic and gravity wave-driven ionospheric dynamo phenomena following natural hazard events [e.g. Aoyama et al., EPS, 68, 2016; Toh et al., JGR, 116, 2011]. Particularly, the connection between acoustic wave-generated currents with magnetic perturbations were found after several severe earthquakes [Iyemori et al., EPS, 65, 2013; Hasbi et al., JASTP, 71, 2005]. Moreover, modeling results showed good agreement with observed fluctuations of the geomagnetic field at the ground level [Zettergren and Snively, JGR, 120, 2015].

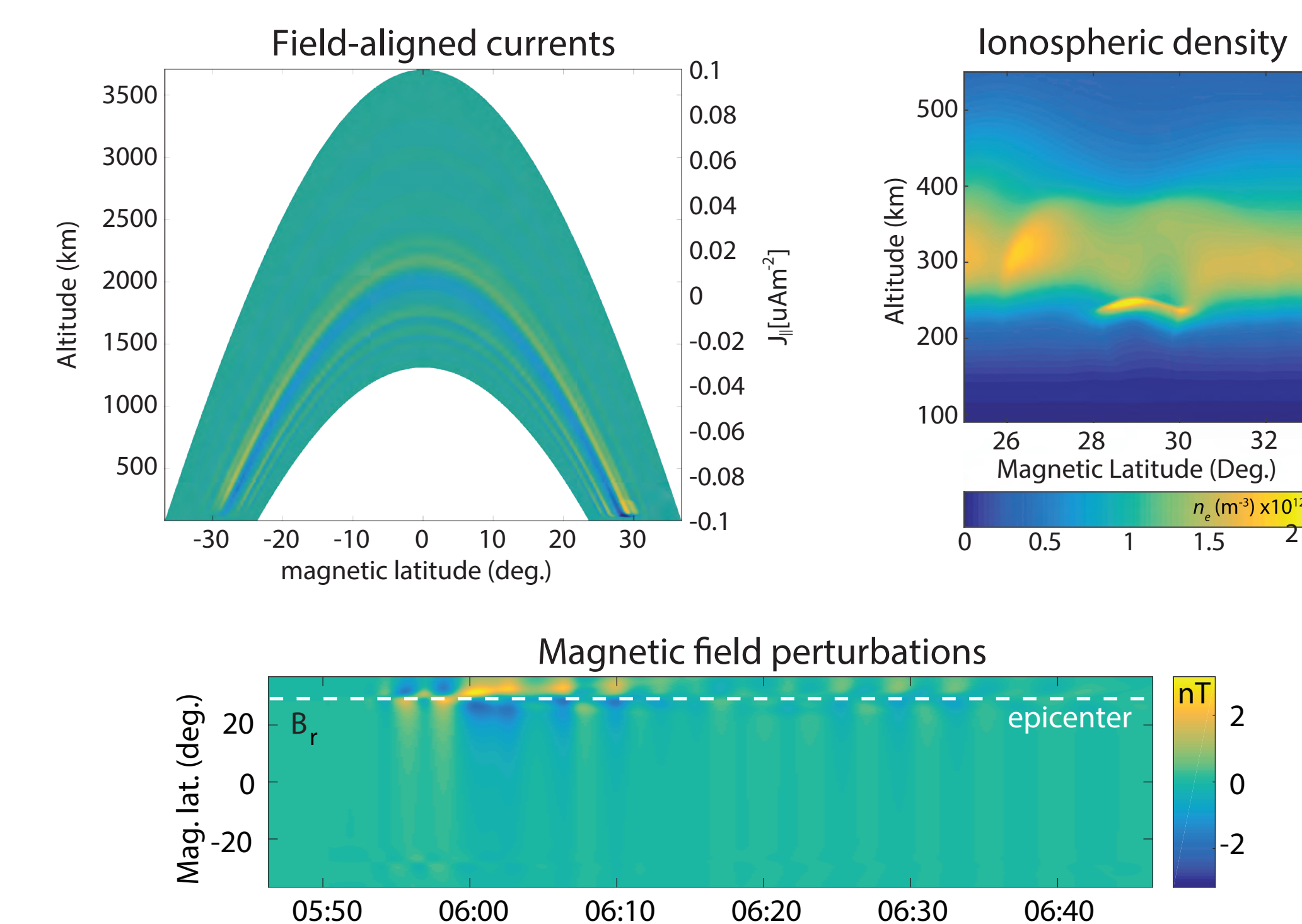
Here, we report comparisons between model and observations based on Zettergren and Snively [2015] and analyses of ground level magnetic field perturbations following the 2010 Chile 8.8M and 2015 Chile 8.3M earthquake events. Iyemori et al. [2013] presented comparisons of barometric and magnetic data following 2010 Chile 8.8M earthquake. The authors interpreted long-period magnetic oscillations (with main peaks at ~190 and 265 sec) as the effect of field-aligned currents generated through a dynamo process in the ionosphere.

In our study, we perform complementary spatial and temporal analyses of the disturbances in ionospheric electron density and magnetic field. Ionospheric total electron content (TEC) data from regional ground-based GNSS receivers and magnetic field data from SAMBA magnetometers network are analyzed. Data from regional networks of seismometers are also utilized to discern magnetic field perturbations caused by surface waves and by acoustic-wave-generated currents. Results suggest that frequencies of perturbations of magnetic field (~4-5 mHz) on ground level appear close to those observed in TEC data, which supports the hypothesis made in Iyemori et al. [2013] indicating that they are due to acoustic wave-generated currents.

Context

TEC measurements based on global navigation satellite system (GNSS) receiver observations are important sources of data to study electron density fluctuations associated with natural hazards. Particularly, acoustic wave periods up to 5 min are often observed in the ionospheric electron density after severe earthquakes, tsunamis, volcanic eruptions, etc. [e.g., Komjathy et al., 2015].

Simulations of ionospheric responses to infrasonic-acoustic waves, generated by vertical accelerations at the Earth's surface, were performed by Zettergren and Snively [2015]. They calculated that the associated magnetic perturbations by the simulated waves are observable and may provide new observational insight in addition to that provided by GPS TEC measurements. This result is also consistent with real magnetic field measurements using satellites data [Iyemori et al., 2015] and ground-based instruments [Hasbi et al., 2009, Hao et al., 2012]. Zettergren et al., [2017] simulated the nonlinear atmospheric and ionospheric responses following the sea surface responses to the Tohoku earthquake, finding both electron density and magnetic field perturbations similar to those observed (see figures below).



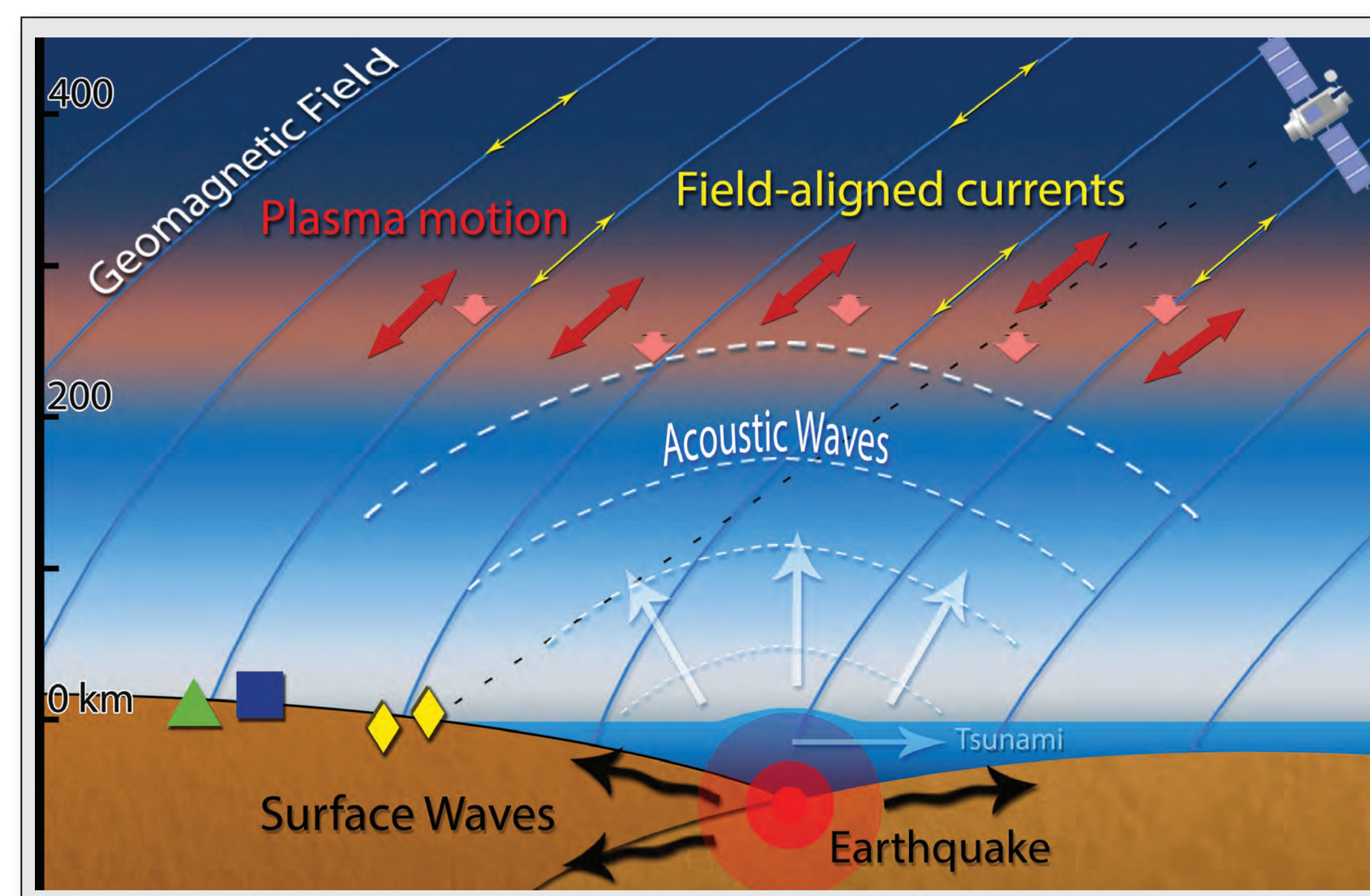
Case studies

Earthquake	Chile 02.27.2010	Chile 09.16.2015
Intensity	8.8Mw Megathrust	8.3Mw
Time	03:34:11 CST (06:34:11 UT)	19:54:33 CST
Coordinates of epicenter	35.9°S / 72.7°W, 3 km offshore	31.57°S / 71.65°W
Tsunami	Yes	Yes

Our present study investigates perturbations of ground-level magnetic field data and TEC measurements following the 2010 Chile 8.8M and 2015 Chile 8.3M earthquakes. We find that fluctuations in magnetic field appear connected in time and consistent in spectrum with ionospheric dynamo currents caused by acoustic waves that are generated by the earthquake. The comparison of real data results and model results supports this hypothesis, and also opens important questions to motivate further investigations of earthquake related magnetic and TEC fluctuations.

EMBRY-RIDDLE
Aeronautical University

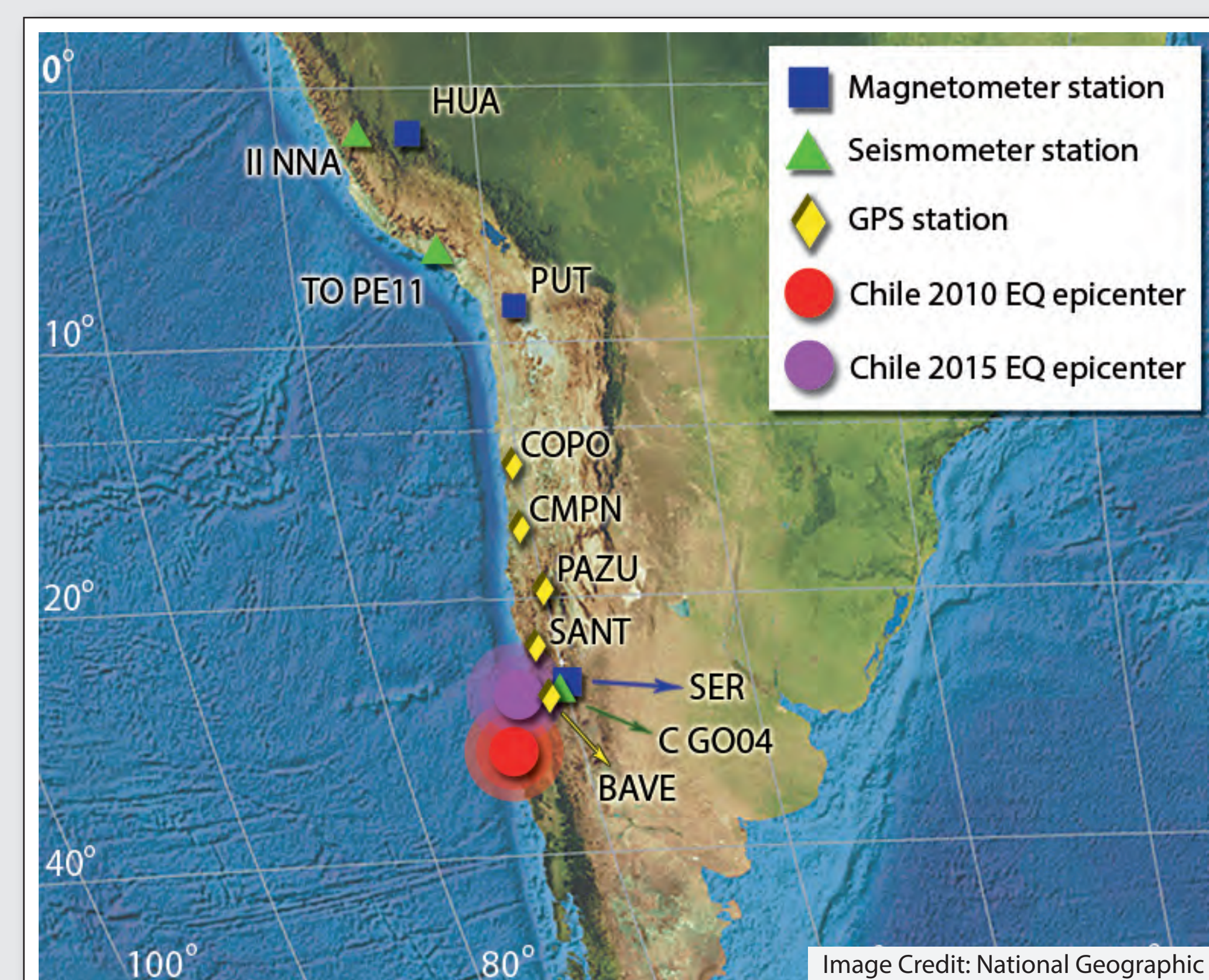
JPL
Jet Propulsion Laboratory
California Institute of Technology



Data description

In this study we used magnetic field data from 3 stations: Putre and La Serena stations in Chile (SAMBA network [Yizengaw et al., 2009]) and Hyancayo, Peru (Instituto Geofisico del Peru [Gjerloev, 2012]). Provided data contains measurements of 3 components of magnetic field with 1 min and 1 s time resolution respectively. Magnetometer data were processed with a 10 min Gaussian moving average filter in order to exclude long-term variations.

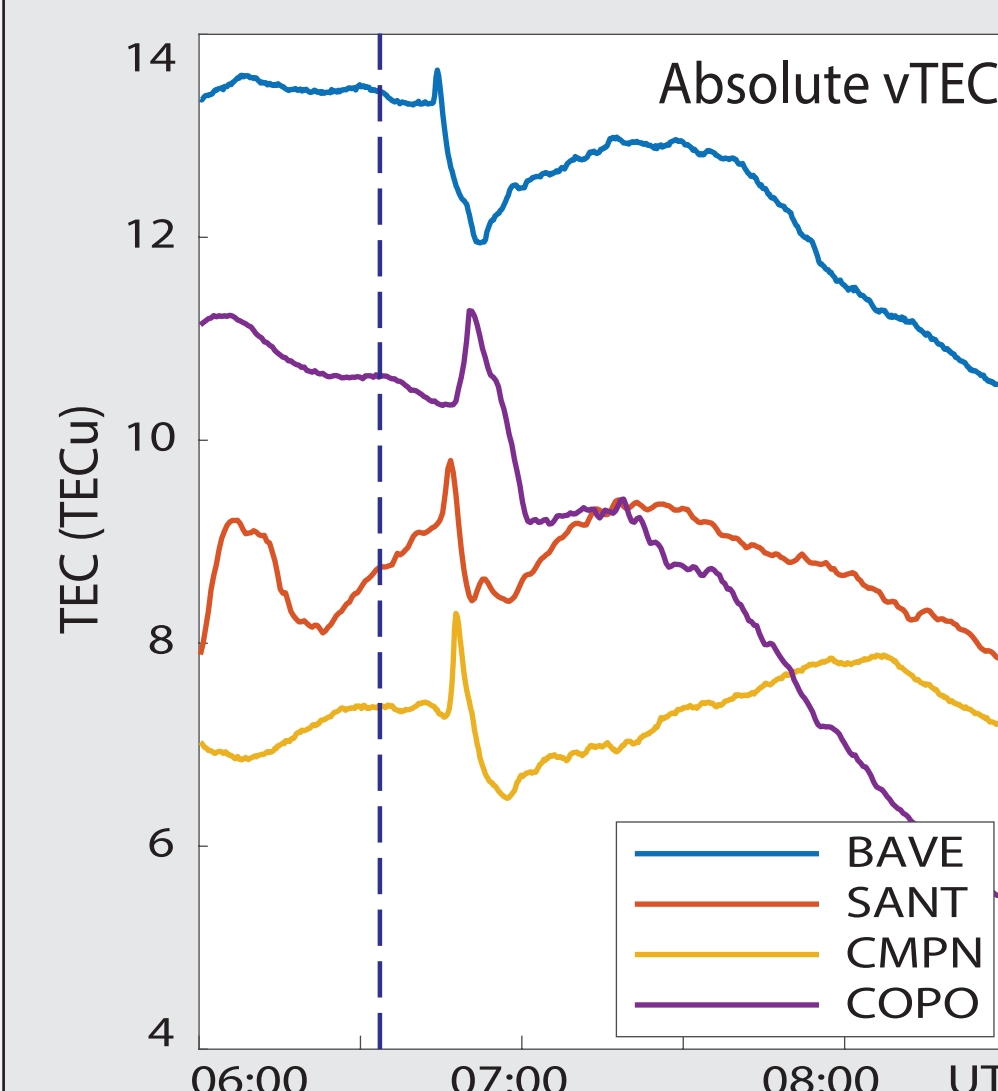
In order to examine influence of magnetic perturbations caused by surface waves and those driven by infrasound dynamo currents, we leverage data from seismometers stations nearby the magnetometers. Seismometer data were received from Chilean National Seismic Network. The analysis is based on the data from High Gain Broadband Seismometers with 1 s (TO PE11), 20 s (II NNA) and 40 s (C GO04) time resolution.



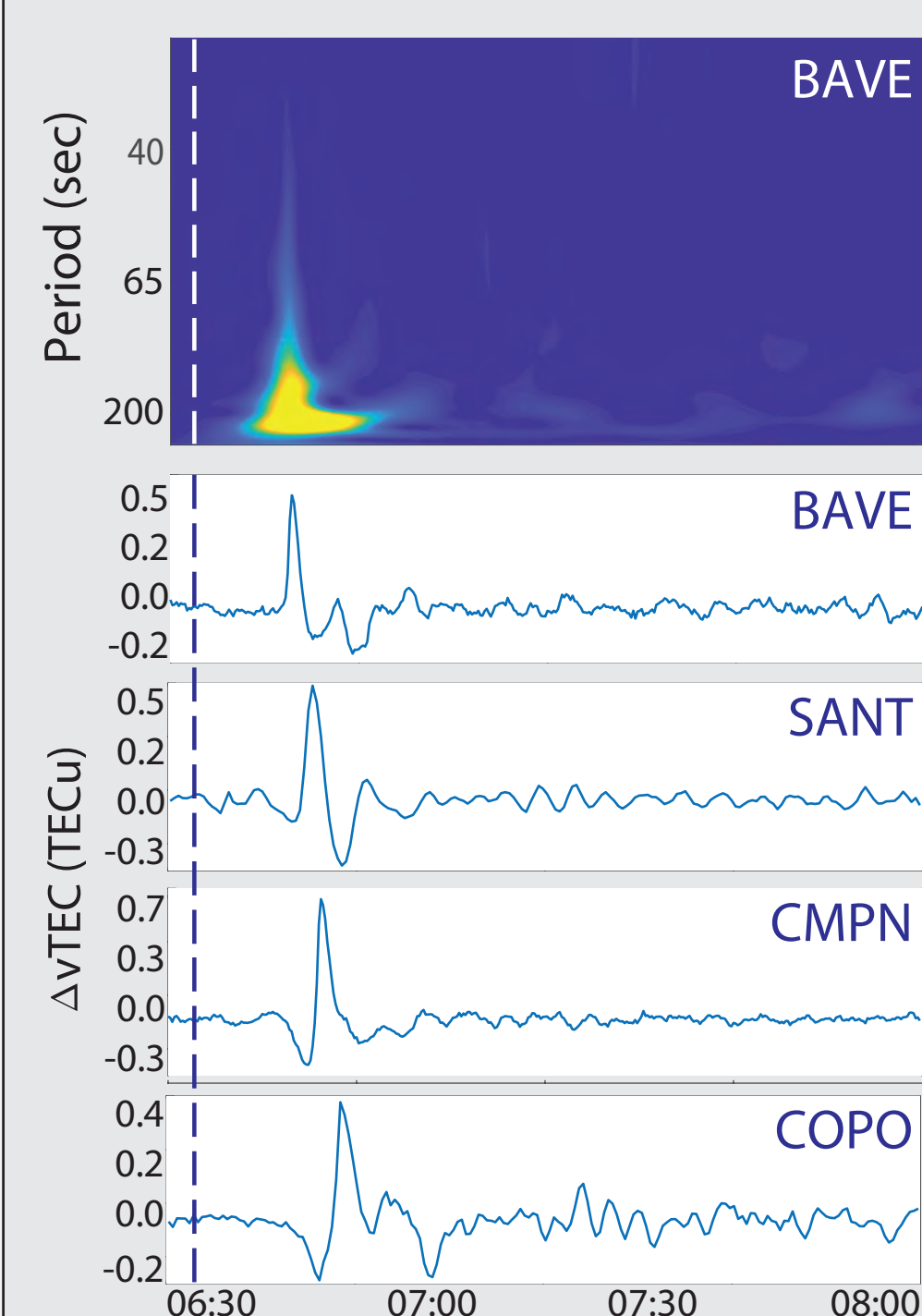
Observations from the ground-based GNSS stations nearest to the earthquake's epicenter, provided by UNAVCO and International GNSS Service (IGS) [Dow et al., 2009] in RINEX (Receiver independent exchange) format, were also analyzed in this study. Calculations of absolute values of vertical Total Electron Content (vTEC) from 30 and 15 sec code and phase measurements on L1 (1.575 GHz) and L2 (1.227 GHz) GPS frequencies for every GPS satellite - receiver line of sight (LOS) were performed. An approximate precision of calculated vTEC is ~0.01-0.1 TECu [e.g., Mannucci et al., 2004]. Among all observations we chose those for which zenith angles between ground stations and GPS satellites were no less than 40°, in order to reduce error connected with low LOS measurements, and those IPP tracks closer to the epicenter.

Chile 2010 8.8M Earthquake

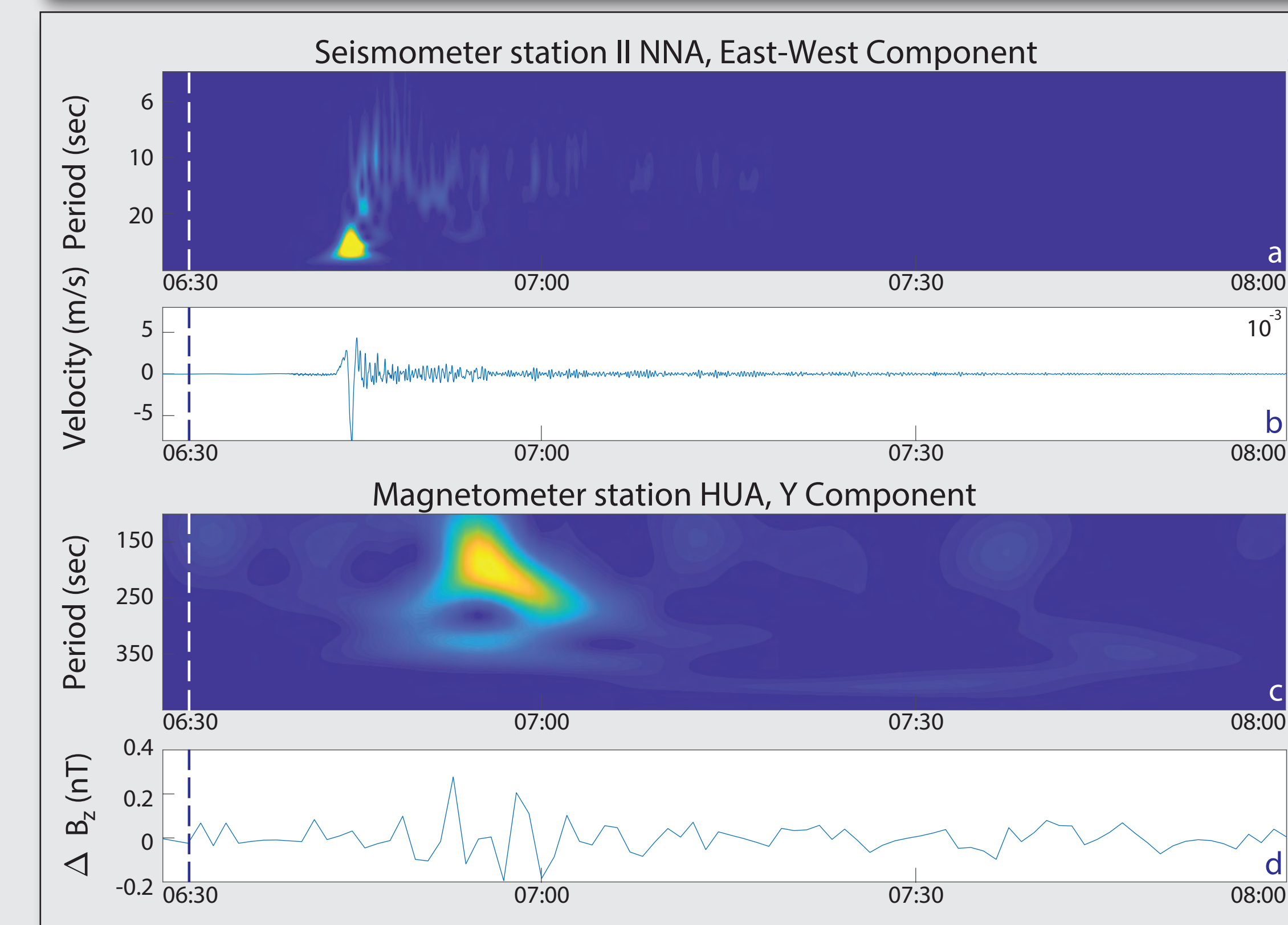
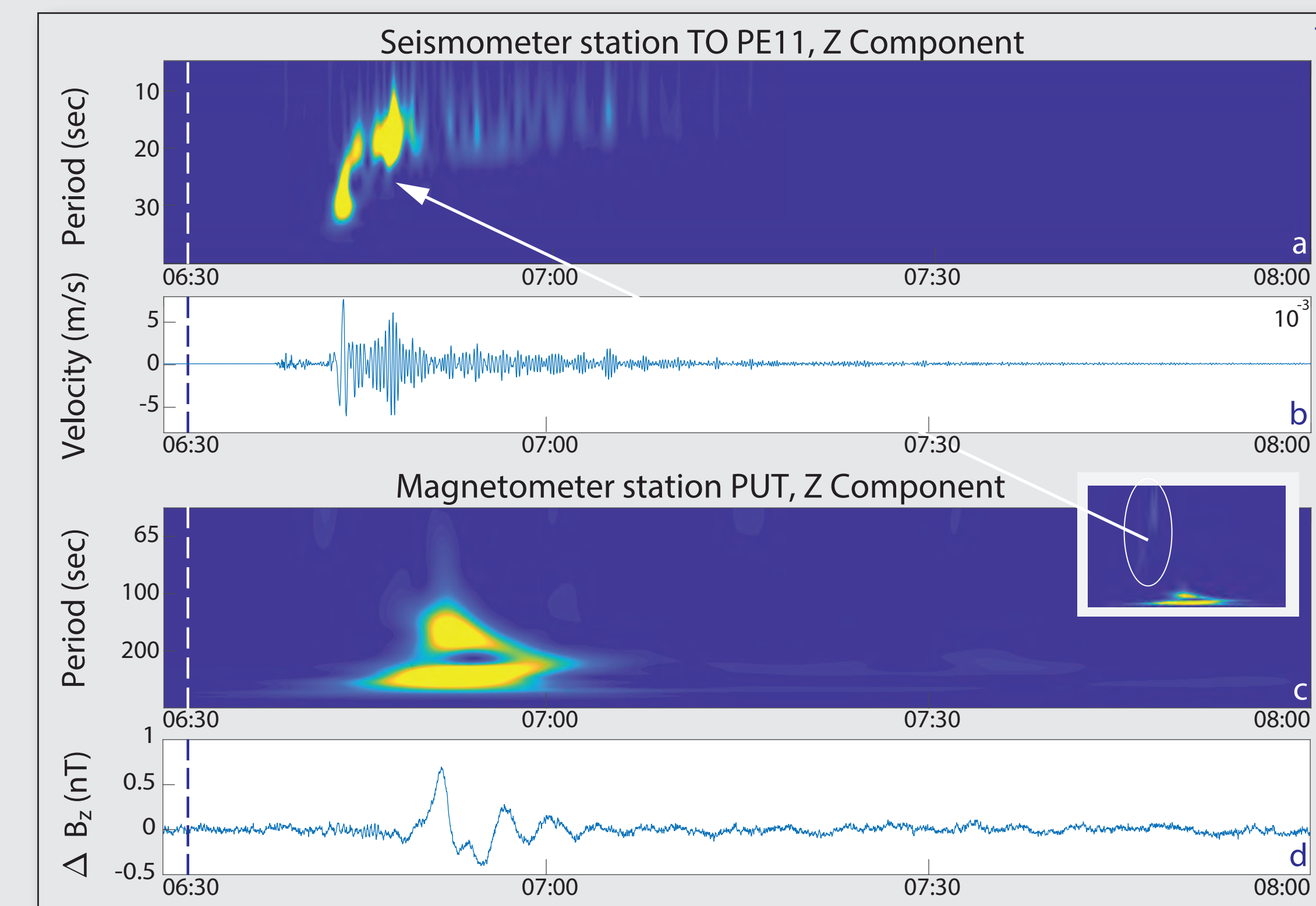
TEC data show sharp perturbations at ~6.45UT in electron density followed by a depletion and recovery lasting ~45 min. Peak to peak variations are up to 0.7 TECu.



Perturbations on seismometers stations TO PE11 and II NNA were firstly registered at 6:40UT and the periods of them were found to be ~20-30 sec. Fluctuations in magnetic field with periods of ~150-250sec are found to be 10 min later - first on PUT station and then on HUA. This is consistent with results presented by Iyemori et al., 2013]. Perturbations of magnetic field were up to 0.7nT in amplitude.

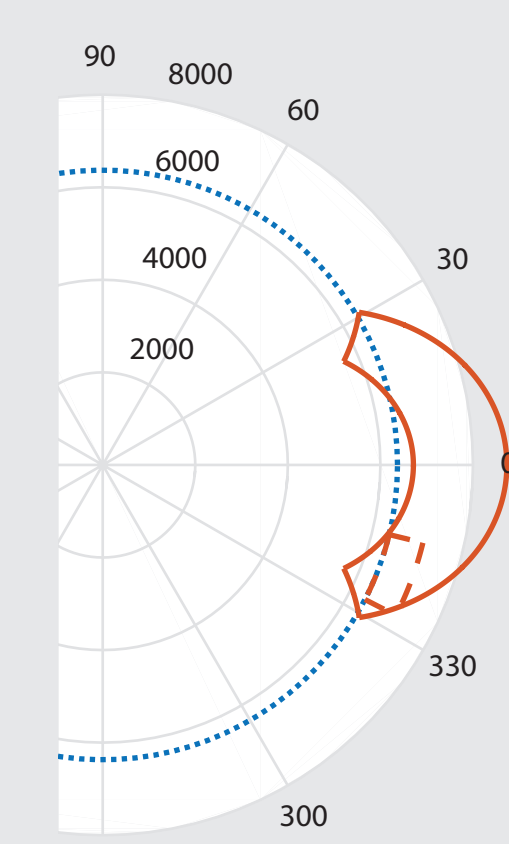


For the analysis of electron density variations connected with acoustic waves generated by the earthquake, absolute values of vTEC were de-trended using 10 min Gaussian window moving average filter in order to exclude long-term fluctuations from other sources and diurnal variations. Analysis showed that perturbations with ~180-270 s periods were registered after ~8 min what is consistent with the speed of propagation of acoustic waves up to height of F2 region of the ionosphere. Spectrograms and time series plots show observable perturbations in TEC data caused by acoustic waves after the earthquake for all 4 chosen GNSS stations.



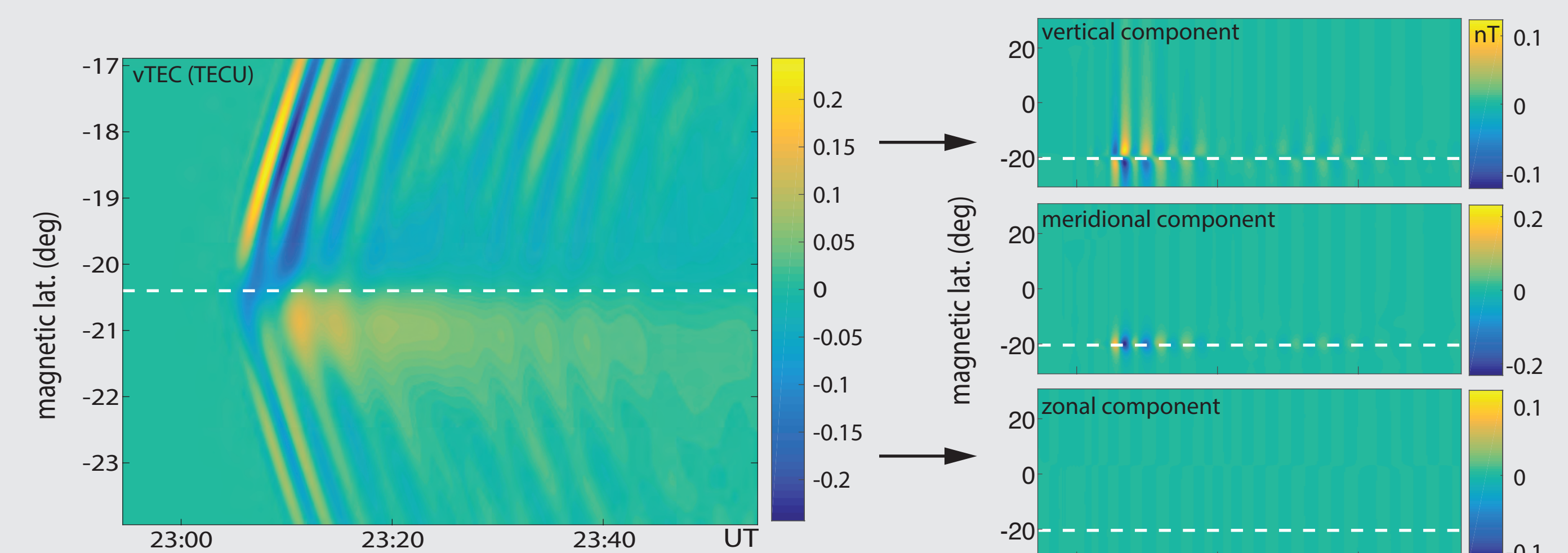
Chile 2015 8.3M Earthquake

Data from C GO04/SER stations were used to investigate responses following the 2015 Chile 8.3M earthquake. The perturbations in magnetic field were found in the Z-component with approximately similar periods as for 2010 case ~250 s (figure 3). This is also consistent with periods of perturbation in TEC data for PAZU station.



The models of Zettergren and Snively [2015] were used to simulate the ionospheric response to ground level forcing of the atmosphere, capturing atmospheric acoustic wave dynamics and the comprehensive ionospheric responses. The overlapping domains for the two grids constructed for the Chile 2015 Earthquake modeling case are presented to the left. Solid lines - the extent of the ionospheric model grid; dashed lines - the extent of the neutral dynamics model grid.

The source used to excite waves within the model is highly simplified, consistent with a sinusoid at 90 second period applied at a peak vertical velocity of 7mm/s at the model lower boundary, with 40 km radial scale. [e.g., Zettergren et al., 2017]. Model results are presented below.



Discussion/Future works:

Results of our present study suggest that magnetic perturbation signatures at ground level can serve as an additional source of information for the analysis of coupling processes and energy flow in the lithosphere-atmosphere-ionosphere system. However, these signatures are not yet well-understood and not yet usable as a quantitative remote sensing tool. Additional well-calibrated modeling will be necessary.

More detailed case studies of the contribution of atmospheric acoustic and gravity waves to magnetic perturbations following strong seismic forcing are planned for the near future. Additional data sources of electromagnetic field measurements will be investigated. In particular, Aoyama et al., [2016] show that such magnetic effects can be observed in topside ionosphere using SWARM satellites data. Systematic parametric modeling of magnetic responses based on typical source information will also be carried out using improved 3D ionospheric models. Finally, wave sources including land and sea surface responses, will be simulated to generate realistic spectra.

Acknowledgements:

The authors thank E. Yizengaw, E. Zesta, M. B. Moldwin and the rest of the AMBER and SAMBA team for the data. AMBER is operated by Boston College and funded by NASA and AFOSR. SAMBA is also operated by UCLA and funded by NSF. Seismometers data were provided by Chilean National Seismic Network through Incorporated Research Institution for Seismology (IRIS) services. The facilities of IRIS Data Services, and specifically the IRIS Data Management Center, were used for access to waveforms, related metadata, and/or derived products used in this study. GPS observations data from BAVE, CMPN, PAZU and COPO stations were obtained using services provided by the UNAVCO Facility with support from the National Science Foundation (NSF) and National Aeronautics and Space Administration (NASA) under NSF Cooperative Agreement No. EAR-0735156. Data from SNT station were provided by International GNSS Service (IGS). HUA magnetometers station data is provided by Global Ground-Based Magnetometer Initiative (SuperMag). Research was supported by NASA grant NNX14AQ39G to Embry-Riddle Aeronautical University. Models used in this study were developed under support from NSF CAREER grants AGS-1255181 and AGS-1151746.

